Journal of Advances in Science and Technology
Vol.23, Issue No. 1 March-2026, ISSN 2230-9659

Impact of Lower Atmosphere and High-Latitude Forcing on Thermospheric Density

Vikash Kumar Singh*

Ph.D. Scholar, Department of Physics, Shree Krishna University, Sagar Road, Chhatarpur, M.P. India

vikashami92@gmail.com

Abstract : During the geomagnetically disturbed period from 31 January to 3 February 2024, this research examines the combined effects of decreased atmospheric forcing and high-latitude magnetospheric inputs on thermospheric neutral density. The work investigates the impact of realistic lower-boundary conditions, specifically those derived from WACCMX-SD, on the global thermospheric response relative to climatological forcing using Swarm-C satellite observations and a number of TIEGCM-based simulations. By using real lower atmospheric disturbances, density errors are regularly reduced, particularly in the northern hemisphere In many latitude zones, reductions of up to 15% have been seen. It is important to have correct representations of the connection between the magnetosphere and ionosphere because models powered by field-aligned currents (FAC) obtained from AMPERE data perform better than those employing empirical Weimer electric fields, especially at night and at high northern latitudes. Results show that complex interactions including circulation patterns, tidal variability, composition variations, and scale height differences based on altitude are the root cause of interhemispheric asymmetries in density response. The research concludes that in order to better model and forecast space weather, it is necessary to take into account both lower atmospheric dynamics and high-latitude energy inputs, since both are crucial in capturing fluctuations in thermospheric density.

Keywords: lower atmosphere, high-latitude forcing, thermospheric density

INTRODUCTION

Atmospheric tides, planetary waves, and seasonal circulation patterns may alter the thermosphere's condition, and fluctuations in geomagnetic activity also affect it. The significance of comprehending this multiscale interaction for satellite drag, orbital prediction, and variability in the ionosphere-thermosphere (IT) system has grown in recent years. [1]

Increased energy intake from field-aligned currents or particle precipitation in the auroral area may significantly change the thermosphere's density, temperature, or composition during geomagnetic storms, according to research. Also, neutral winds and vertical transport are affected by lower atmospheric forcing, which includes both migratory and non-migrating

tides. This causes hemispheric asymmetries and variations in mass density that are dependent on altitude. [2]

These coupling mechanisms can now be more accurately represented thanks to recent developments in whole-atmosphere modeling. The fluctuation of planetary waves and tides may be better captured by data-assimilative models like WACCMX-SD, which, when combined with MERRA-2 reanalysis, provide lower boundary conditions that are more realistic than climatological ones.[3]

This period is perfect for testing the relative contributions of lower atmospheric drivers and magnetospheric forcing because the Swarm-C satellite detected substantial density enhancements and clear hemispheric differences during the moderate geomagnetic disturbance from 31 January to 3 February 2024, which NOAA classified as a G1 storm. [4] During this time, Swarm-C was in an orbit of 450–478 km, a region where atomic oxygen is abundant and where differences in density may be detected due to tiny changes in wind-driven transport. [5]

Although this trend flipped in certain daylight low-latitude locations, demonstrating complex seasonal and dynamical interactions, observations indicated that neutral density in the Southern Hemisphere was 30% greater than the Northern Hemisphere during nighttime orbits. [6]

The study's objective is to ascertain the relative contributions of each driver to the observed fluctuations in neutral density by comparing several TIEGCM simulations that include climatological and WACCMX-SD lower bounds in addition to Weimer and AMPERE-derived high-latitude forcing. [7] To enhance thermospheric modeling, this method clarifies interhemispheric disparities, reactions that vary with altitude, and the processes that lead to simulation mistakes.[8]

METHODOLOGY

The neutral density from 31 January to 3 February 2024, a moderately geomagnetically disturbed interval, was examined and how lower atmospheric and high-latitude forcing influenced it. This is a modest G1 on the NOAA Space Weather scale, but it is nonetheless notable. Due to mesoscale magnetosphere-ionosphere coupling events, "Next Generation Advances in Ionosphere-Thermosphere Coupling at Multiple Scales for Environmental Specifications and Predictions" focused on this period. This work aims to uncover the impact of lower atmospheric forcing with high-latitude magnetosphere forcing, after an initial data-

model comparison that revealed significant hemispheric disparities in the simulation outcomes for obtaining the Swarm neutral mass density readings. This research made use of TIEGCM models and Swarm-C neutral density assessments.

Below is a summary of the weather and climate for the period from January 30 to February 3, 2024. Starting at 5 nT, geomagnetic activity begins around the end of January 30. On January 31, a few hours later, the IMF Bz moves south and stays south until 1 February (doy 32) six UT. IMF On 2 February (doy 33), the usual By and Bz swings occur, but on 3 February, at approximately four UT, there is a long-lasting southern IMF Bz phase that begins late and continues for a few hours before moving northward. As on January 31st, the Sym-H index, which is a measure of the symmetric ring current's strength, will be in the negative state until February 1st. Recuperation occurs on February 2nd, followed by another disturbance on February 3rd.

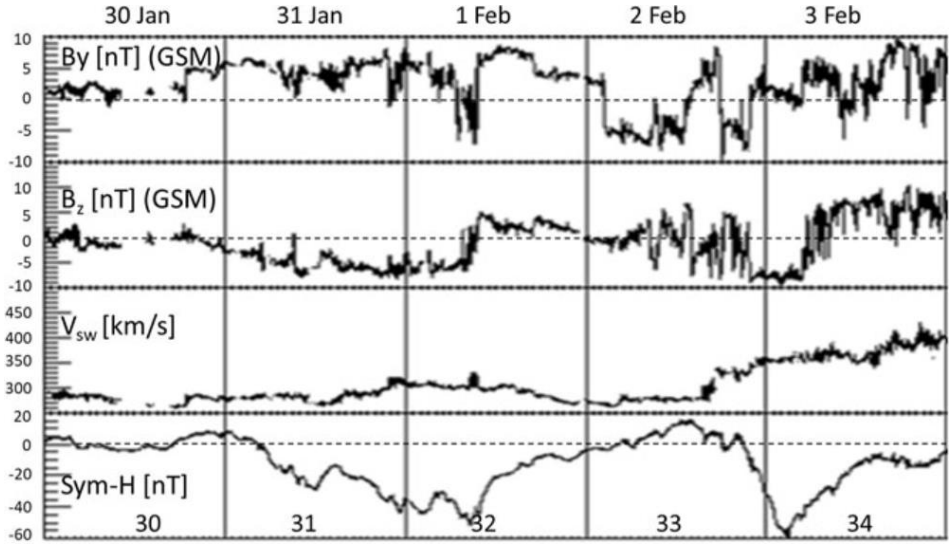

Figure 1: Dates and weather forecasts for January 30–February 3, 2024 (1924

Neutral Density of A Swarm

A four-step Swarm data product (DNSxACC version 0201) by Siemes et al. (2016) provides neutral density [9]. Until then, Swarm-C orbits about 450-478 km. South-bound high-latitude orbits are 20 kilometers higher than north-bound. NRLMSIS2.0 says lower altitudes have 1.4-5 times greater neutral density. In medium to low latitude orbits, overnight is 2.5-3 hours SLT and daylight is 14-15 hours. Figure shows the average sun zenith angle lighting the southern polar region at night. An angle darkens the northern hemisphere.

Methods for comparing neutral density emphasize different variance features. Neutral density may be measured globally, orbitally, relative, absolute, and altitude-scaled. To eliminate scaling bias based on common height, use the orbit's neutral density.

With no more than two orbits per bin, observed neutral density is likely more accurate than calculated, which uses 2 hours and 4 degrees of geographic latitude bins. Doy 32 and 34 have high geomagnetic activity, raising neutral density. However, at low and medium latitudes, the neutral density is not necessarily larger in the NH than in the SH.

Distinct variations in neutral density between the 2 hemispheres may have several causes. Variations in the sun zenith angle throughout the year cause neutral dynamics & composition to vary throughout the hemispheres. Swarm orbit altitude differs between SH summer and NH winter, which counteracts the seasonally increased neutral density in the former. Furthermore, the neutral density and thermospheric and ionospheric states may be altered by the reduced atmospheric forcing, which includes its own intrinsic seasonal fluctuation. The increased energy input from high latitudes into the IT system during geomagnetic storms might cause hemisphere variations. To model the neutral density fluctuations using TIEGCM, we will examine the role of forcing at lower atmospheric and upper latitude levels.

TIEGCM

Incorporating thermosphere and ionosphere energetics, chemistry, and atmospheric dynamics, the TIEGCM achieves self-consistency. Implications from magnetosphere-ionosphere coupling, the wind dynamo, and the current produced by gravity & plasma pressure gradients constitute the TIEGCM's ionospheric electrodynamics.

Its range depends on solar cycle conditions, from 97 to 450–600 kilometers. We utilize 2.5o x 2.5o horizontal resolution for global latitude and longitude. An analytical auroral model defines cloud particle precipitation in both circumstances. Weimer and FAC driven models updated the default TIEGCM auroral parametrization, as seen in the first supporting document. This section shall refer to the Weimer-driven simulation as "Weimer" & the field-aligned current-driven simulation as "FAC."

The two hemispheres' high latitude FAC patterns are generated by principal component analysis of Iridium satellite AMPERE magnetic field observations. The FAC distribution is smoother than the AMPERE field-aligned current since less PC are used. Compared to AMPERE FAC, PC-based FAC has a lower hemisphere combined up and down FAC measure.

By increasing the FAC magnitude in both sides by 45%, we may attain hemispheric integrated FAC intensities comparable to the initial AMPERE data.

The three-step process for determining electrostatic potential... The electric potential is first determined by the global wind dynamo and the hemispherically symmetrical FAC component. Using either the local wind dynamo or the symmetric potential solution from step 1, the FAC at the top of the ionosphere in each magnetic hemisphere is calculated in step 2. In the third phase, for each hemisphere, utilize the computed FAC minus the given FAC. In Step 2, the FAC is computed at the upper boundary at high latitudes, and in Step 3, the zero potential restriction is determined at the equatorwards border (here at $|40^0|$ magnetic latitude). Repeat for each hemisphere. After stages 1 and 3, a magnetic grid has symmetric and asymmetric potentials. To calculate electric potential, add steps 1 and 3. To balance ionosphere current, the FAC must be modified at each level.

We can explain background variations and disturbances in horizontal wind, neutral temperature, or geopotential height at the TIEGCM LB, about 97 km. We run two simulations to determine how decreasing atmospheric forcing affects neutral density. We employ a climatological LB baseline or perturbations in one simulation. The MSIS00 model & HWM07 horizonal wind model establish the LB background, while we employ GSWM tidal climatology. GSWM includes diurnal, semi-diurnal, and non-migrating tidal components. The mid-month TIEGCM describes and interpolates hourly GSWM perturbations chronologically. This simulation is labeled "Climate".

A TIEGCM simulation is compared using WACCMX-SD LB. Surface and thermosphere climate model WACCM-X includes complete atmosphere. WACCM-X dynamics are pushed up to 50 km toward reanalysis data like Modern-Era Retrospective analysis for Research & Applications, Version 2 to model certain time periods. WACCMX-SD data at the TIEGCM LB may reveal the background "B" & perturbations "P" throughout this time, including planetary waves and tides. We employ WACCMX-SD output at the pressure level closest to the TIEGCM LB to study the neutral density change caused by a more realistic background environment and the lower boundary perturbation. Baseline: geopotential height, neutral temperature, daily zonal & diurnal horizontal wind mean. By removing background from total fields, perturbation fields result. "WacXBP" is the LB WACCMX-SD simulation. Simplify the "Climate" simulation using the climatological baseline (CB) & WACCMX-SD

perturbations (WacXP) as "WacXP-CB" case study. Every simulation uses the TIEGCM, although they handle forcing at the lower boundary and high latitudes differently.

Using the 3-hourly Kp index-generated high latitude electric potential and suitable lower boundary forcing, all of our simulations start on day 10, 2024. High latitude forcing simulations were resumed from day 30. Using the same binning approach, we compare the synthetic data to the TIEGCM simulated neutral density for the Swarm-C orbit. For all time, the TIEGCM's upper boundary has been higher than Swarm-C's orbital height. The sum of the absolute differences (L-1 norm) of the binned data is used to compare the simulated and actual neutral densities, rather than the root mean square error, which weights by error size. The entire Swarm-C neutral density fluctuations are used to determine comparative errors unless otherwise stated.

RESULTS

Implications of reduced atmospheric forcing

First, we compare simulations utilizing climatological forcing at the lower boundary and WACCMX-SD (WacXBP) to investigate how lower atmospheric forcing impacts neutral density at Swarm-C altitude. The high latitude FAC force is same in all cases. The graphic shows that Climate & WacXBP simulations of the Swarm-C neutral density for both nighttime and daytime orbits were wrong.

At night, neutral density error is larger than during the day. NH has a higher daytime simulated neutral density. Everywhere except north of 60 degrees south, nighttime simulated neutral density is overestimated. The neutral density error is not increased by the doy 32–34 unrest.

Compare the Climate simulation to the WacXBP simulation in Figure. More realistic LB fluctuations decreased inaccuracy, especially in NH. The southern hemisphere's mid- & low-latitudes have substantially lower nighttime inaccuracy than daytime. Neutral density in the southern polar area is consistent throughout the simulation.

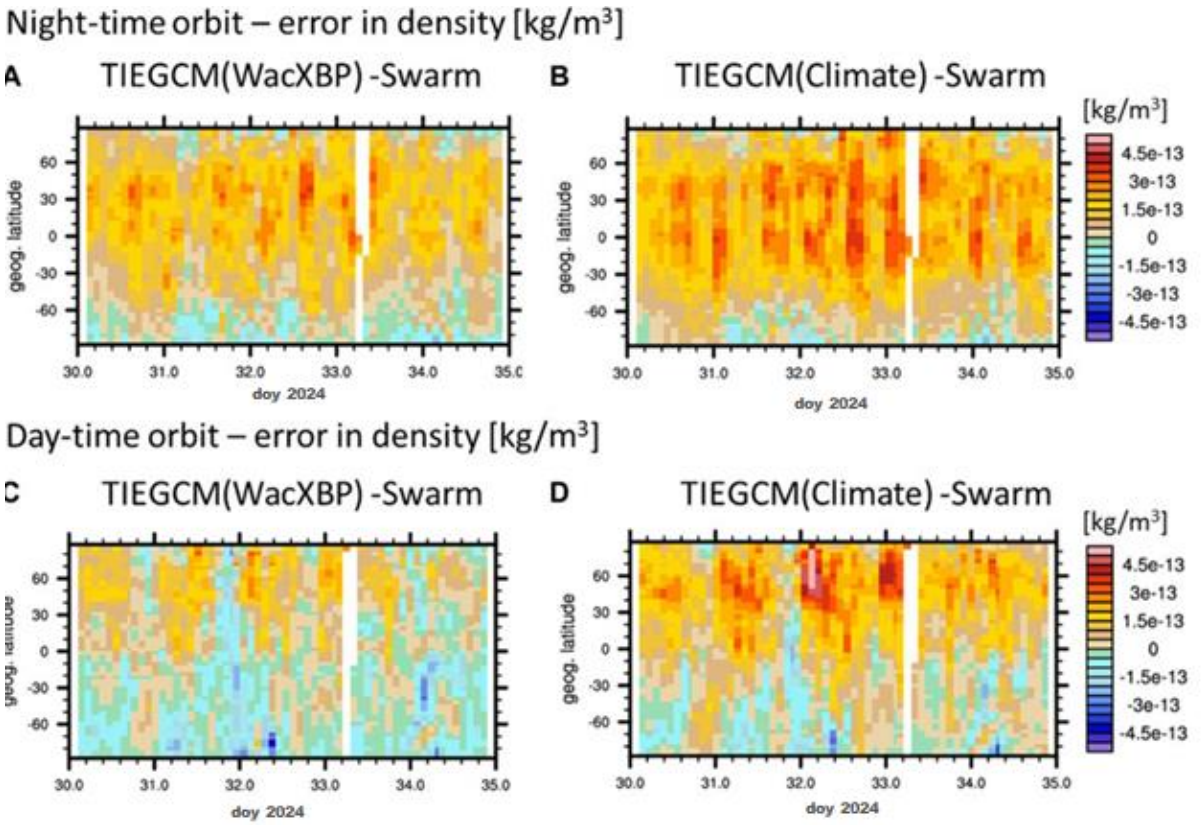

Figure 2: Differences in neutral density between TIEGCM(WacXBP) or Swarm-C & TIEGCM(Climate) & Swarm-C, as well as variations in the neutral density's daytime and nighttime orbits

We narrow the emphasis in Figure to the average fluctuation in neutral density over certain latitudinal regions in order to simplify the findings. Typically, the discrepancy is more pronounced after the sun goes down. When comparing the WacXBP and Climate simulations for the shown northern hemisphere scenarios, the former shows less inaccuracy overall; however, this improvement is less pronounced at night. When comparing the WacXBP and Climate simulations, the difference in the northern hemisphere is around a 15% reduction in inaccuracy. We cannot rule out the possibility that LB conditions from other years with comparable variability might provide similar findings, even if the climatology outperforms the WacXBP simulation using the wave spectrum from the February 2024 timeframe when it comes to capturing the neutral density. This is beyond the purview of the present investigation, which is concerned with the significance of the lower atmosphere & extreme latitude forcing in general.

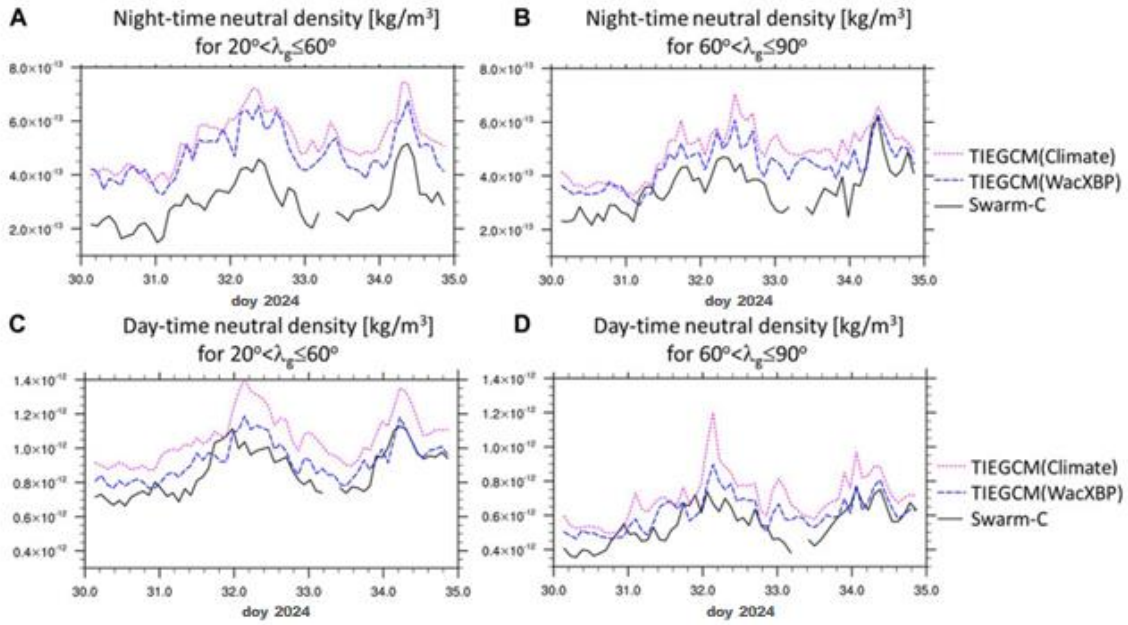

Figure 3: Swarm-C, TIEGCM(WacXBP) , & TIEGCM changes in neutral density over the northern hemisphere's latitudes.

Find out why the NH boosts neutral density more than the SH by dissecting the models. In the lower thermosphere, the Climate and WacXBP models show unique 5-day averaged zonal mean wind patterns at 120 km about doy 30-34. The main points will be supported by a simplified diagram. The climate model's thermosphere circulation has a summer-to-winter cycle, with raising in the south (beyond 20 S), going north, and dropping in the north (beyond 70 N). The WacXBP model has a slightly greater average speed near the poles and a lower southern hemisphere speed beyond 70 S, below 120 km.

The two models' circulations over 140 km are comparable in summer and winter. The Climate simulation changes temperature and composition, whereas WacXBP has greater circulation. Figure displays average zonal mean neutral temperature for a 5-day period (doy 30-34) between 200 < |λg| 60o. WacXBP in the SH has lower temperatures than the Climate simulation above 150 km because to upwelling and adiabatic cooling. The WacXBP model forecasts higher North Atlantic temperatures owing to downwelling, but the climate simulation predicts a cooler thermosphere.

The WacXBP simulation's southern hemisphere is warmer than the Climate simulation's below 140 km, perhaps due to greater downhill or no upward circulation. Temperature and mean circulation alter neutral density and composition. The neutral density is more impacted

by N2 than O1 below 180 km. In the southern hemisphere below 140 km, WacXBP has a lower N2 number density than Climate. This is because the former transports N2 from locations with greater number densities towards greater altitudes with an upward pace, whereas the later does so at a downward rate. At these altitudes, the WacXBP scenario has a lower neutral density in the southern hemisphere than the Climate scenario due to less N2 in the lower thermosphere.

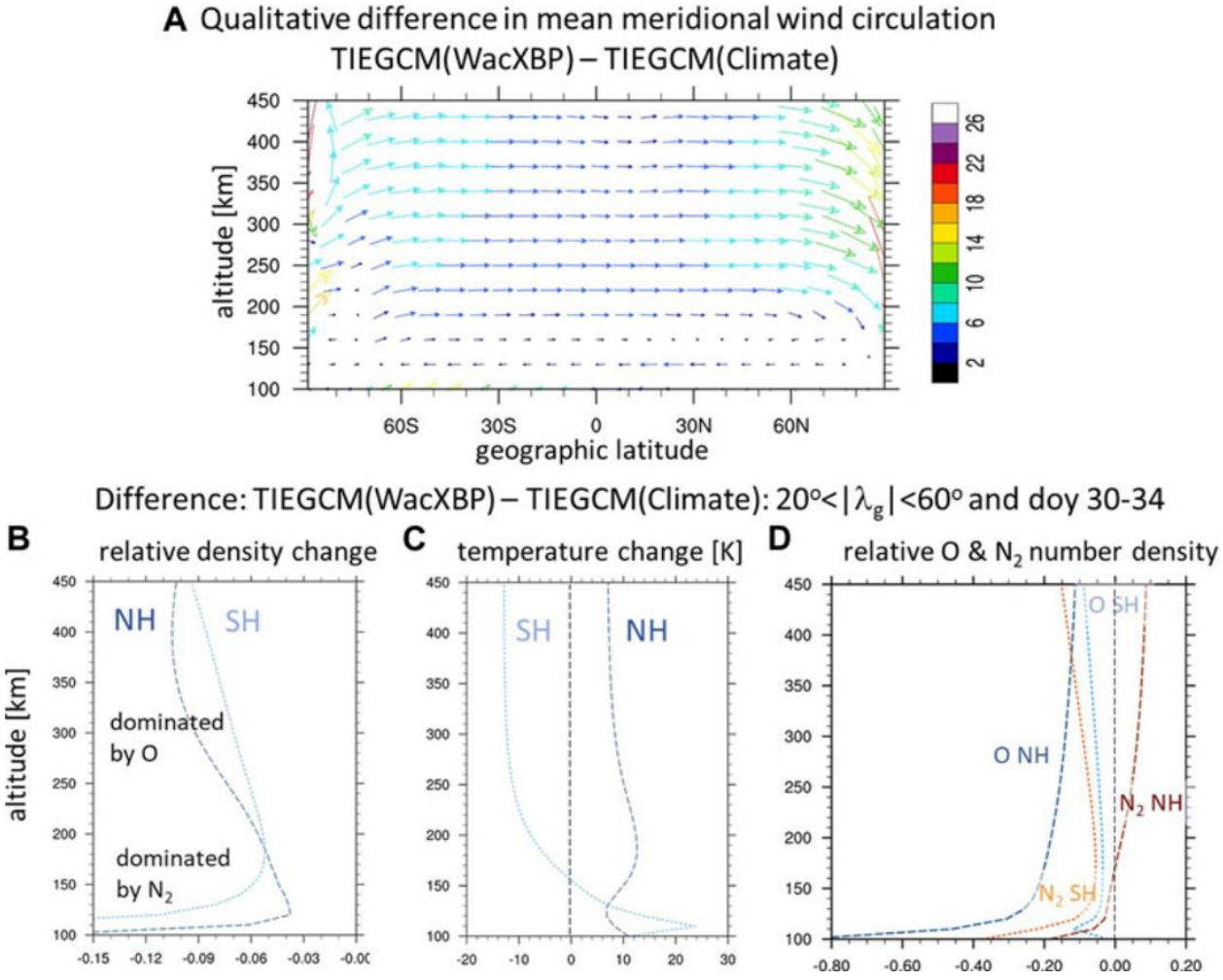

Figure 4: (A). Doy 30–34 TIEGCM(WacXBP) vs. (Climate) (A). diurnal and zonal mean circulation (B–D). TIEGCM(WacXBP) & TIEGCM(Climate) show average changes across 20o < |λg| ≤ 60o and doy 30–34 at altitude (B). neutral density vs. TIEGCM(WacXBP); K (D) temperature. Comparing O & N2 number density to TIEGCM(WacXBP).

Lower altitude circulation in the northern hemisphere is not different in the models. The WacXBP example has a lower neutral density at these altitudes than the Climate simulation due to enhanced tidal variability and air mixing.

At 450 km swarm heights, atomic oxygen should dominate. Summer has a greater scale than winter, hence vertical gradients in O1 density are fewer in southern summer than northern winter. Because the northern winter hemisphere has bigger vertical gradients, the LB boundary's vertical velocity fluctuations will affect number density more than in the southern summer. Due to stronger downwelling, WacXBP lowers O1 more in the northern hemisphere than Climate. Because O1 transfers better to high-recombination locations. Since WacXBP has a larger scale height in NH than Climate, altitude reduces the absolute difference in O1 number density.

As in the NH, the SH had a smaller absolute change in O1 number density between Climate or WacXBP models. In the WacXBP model, vertical winds and tidal variations may boost air mixing. The Climate simulation has a higher southern hemisphere mean temperature & scale height than the WacXBP simulation, although their absolute O1 number density disparity grows slowly with altitude. Southern hemisphere neutral density differences grow roughly linearly with altitude in Climate & WacXBP simulations, although they are lower than the NH difference between 200 & 470 km. At the end of the simulation, decreasing boundary forcings should induce equal O1 number density changes in the southern & northern hemispheres at altitudes above 450 km.

The models predict a maximum interhemispheric difference of 350 km in the upper thermosphere, which varies with height and the neutral density response to lower atmospheric forcing. At an altitude where NH reacts more to LB changes than SH, Swarm-C is above the maximum differences.

We examine the effects of LB disturbances and backdrop on the IT system by substituting the WacXB background with the climatological LB background from CB. The WacXP-CB and WacXBP simulations vary because to LB background force variation. Based on other research, LB perturbations are more relevant than background forcing.

Quantitative study does not explain how the hemispherically asymmetric component of WACCMX-SD perturbations creates the response difference between the hemispheres. LB perturbations are necessary to replicate large-scale neutral density Geopotential height, LB symmetric zonal wind, & antisymmetric meridional winds are simulated. In most instances, the southern-northern error gap increases when the LB is not interrupted symmetrically. The WacXBP simulation may have 2% lower SH error and 8% higher NH error. Understanding

how the two pieces react requires further research. Asymmetric LB perturbations partially cause hemisphere neutral density disparities, according to simulations.

Influence of high-latitude temperatures

When studying local and regional effects in the thermosphere and ionosphere, in particular the cusp neutral density improvements, it is crucial to have precise measurements of the magnetospheric energy input into the IT system. The importance of a more accurate depiction of forcing at high latitudes to the large-scale reaction at low and medium latitudes is less apparent. Hence, we will contrast FAC simulation based on AMPERE data with the empirical Weimer in the following. At the TIEGCM lower boundary, WACCMX-SD forcing is applied in both simulations.

The neutral density error as it relates to both the simulations and the Swarm-C data varies with latitude and time, as seen in the figure. In the northern hemisphere, TIEGCM(FAC) often performs better than TIEGCM(Weimer), particularly at night, with a decreased neutral density error of up to 7%-20%. Daytime neutral density errors in northern middle latitudes are comparable for TIEGCM(FAC) & TIEGCM(Weimer). In the southern hemisphere, the TIEGCM(Weimer) simulation exhibits somewhat fewer errors of 1-3% compared to TIEGCM(FAC), but, TIEGCM(FAC) improves the night-time orbit neutral density agreement with Swarm-C.

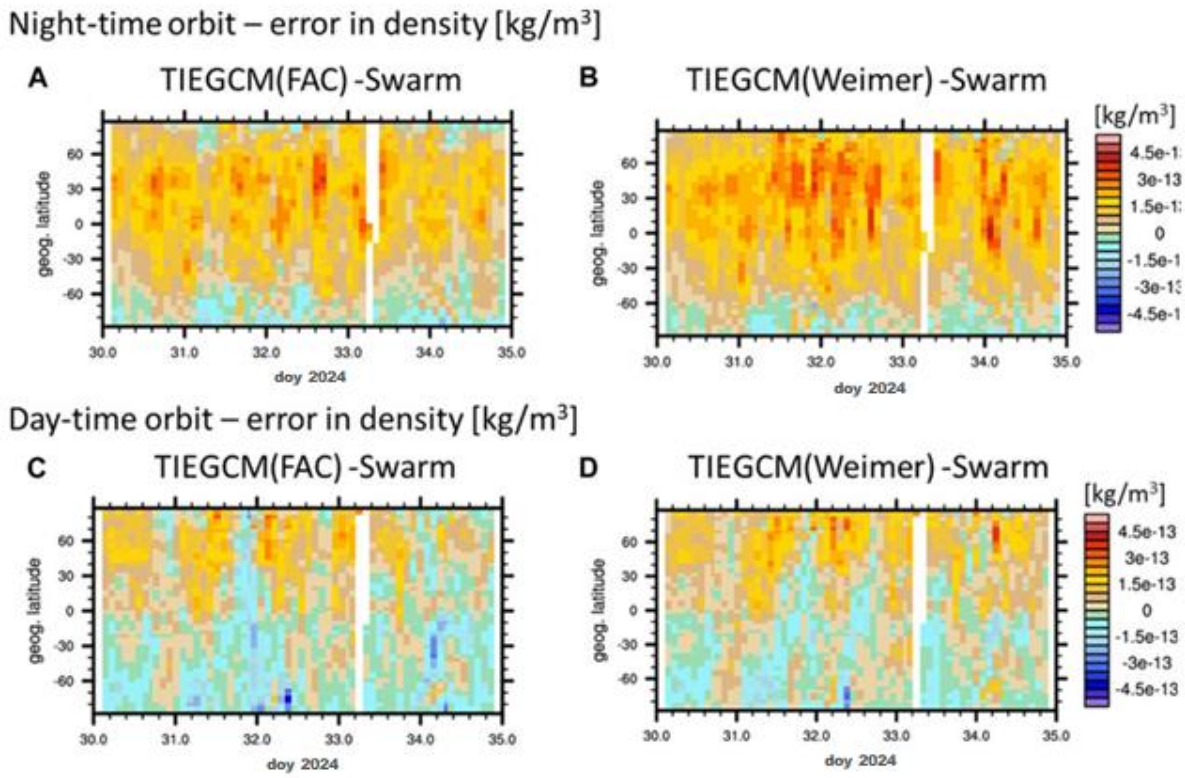

Figure 5: neutral density difference between TIEGCM(FAC) and Swarm-C (A) & (C) and TIEGCM(Weimer) & Swarm-C (B) and (D) for night-time & day-time orbits, respectively.

In the night-time orbit, the neutral density error is bigger in the northern hemisphere than in the southern, as demonstrated by the fluctuation poleward of |60°| geographic latitude. Switching from Weimer to FAC forcing causes greater neutral density changes and enhancements in Swarm-C orbit in the northern high latitudes, especially at night, than in the southern sector. In response to high latitude forces, the models' varying Joule heating across the hemispheres cannot explain the observed hemispheric discrepancy. Figure shows the TIEGCM(FAC) or TIEGCM(Weimer) models' hemispheric integrated Joule heating difference. Both models reveal that the IT system's Joule heating input from the northern & southern polar regions differs.

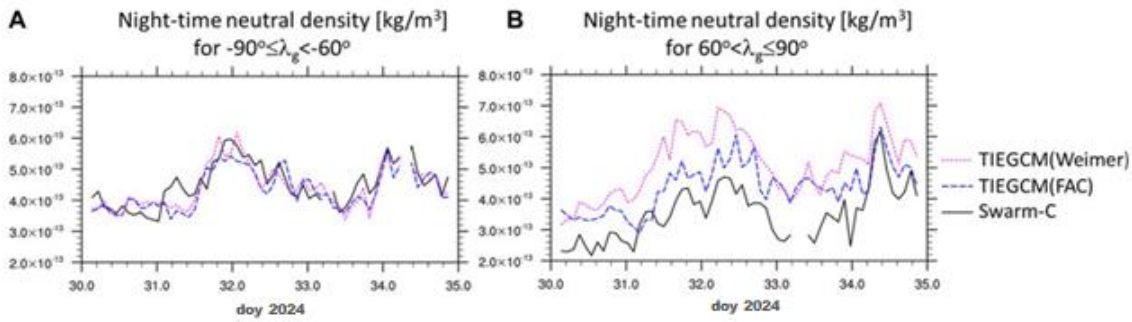

Figure 6: Swarm-C, TIEGCM(FAC), and TIEGCM(Weimer) throughout the night, with large average neutral density changes over the length of the sky

The neutral density and Joule heating discrepancies across the hemispheres are difficult to connect. The northern and southern hemisphere models have a modest relationship in neutral density & hemispheric integrated Joule heating (r = 0.45 and r = 0.3, respectively) even with a time lag. Please note that the 100 GW anomaly in Figure from doy 31.5 to 32.0 accounts for 40-50% of the total hemispheric integrated Joule heating from the TIEGCM(Weimer) and practically 100% of the TIEGCM(FAC).

The neutral density difference is larger in the northern high latitude zone than in the southern high latitude zone for the same Joule heating differences, hence we concentrate on average values poleward of 60^{o} geographic latitude at 3 hours SLT for doy 31.5 to 32.0. In this time period, the SH has a smaller neutral density differential than the NH, but their hemispheric integrated Joule heating differences are similar.

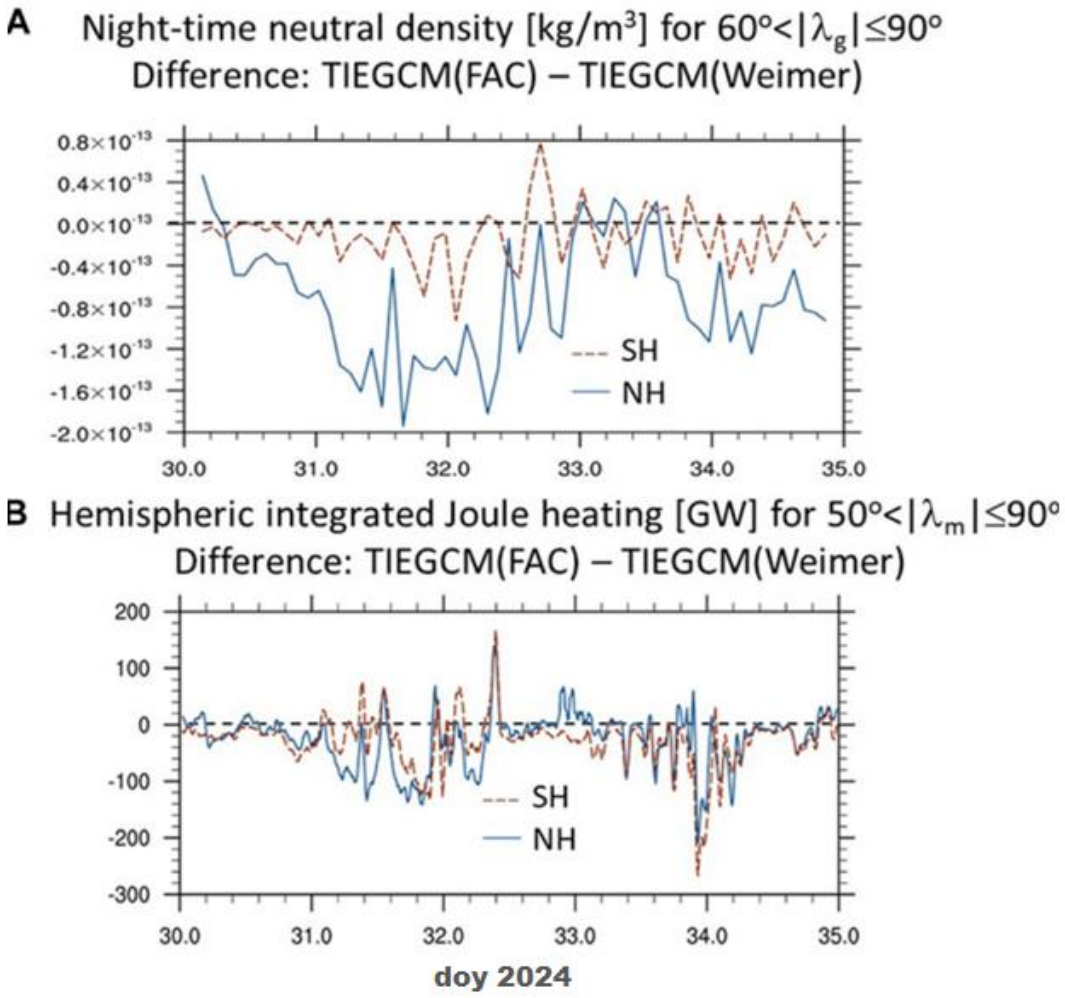

Figure 7: D**ifference. Night-orbit high latitudinal averaged (600 < |λg| ≤ 900) neutral density [kg/m3] difference between TIEGCM(FAC) and (Weimer) and (B). height & high latitudinal integration (500 < |λm| ≤ 900) TIEGCM(FAC) & TIEGCM(Weimer) northern & southern hemisphere joule heating rate [GW].**

The higher thermosphere has a larger neutral density difference between NH and SH, as seen in Figure. The dark winter hemisphere is more affected by Joule heating because the neutral temperature change in the NH is larger than in the SH for the same heating difference. Figure also shows that the TIEGCM(Weimer) simulation has a slightly higher integrated Joule heating value in the NH than the TIEGCM(FAC) simulation, and that the NH dissipates energy more efficiently at higher altitudes (above 120 km) than the SH, where it can change the atmosphere or neutral density. The results below compare 2-4 and 3 hours SLT.

Figure shows how much the simulations differ compositionally. A positive neutral mass density difference exists below 150 km because the N2 number density in TIEGCM(FAC) is

greater than in TIEGCM(Weimer) in the NH, or this difference is larger than in the SH. Both northern & southern hemispheres have positive atomic oxygen differences below 340 kilometers. In the northern hemisphere, atomic oxygen levels reach 340 km, however TIEGCM(FAC) has lower values than TIEGCM(Weimer) owing to its smaller scale height. TIEGCM(FAC) northern hemisphere N2 number density falls with altitude over 150 km compared to TIEGCM(Weimer). Since the NH neutral density difference is practically constant in altitude between 180km & 230km, the positive atomic oxygen difference may explain why TIEGCM(FAC) reduces N2 number density faster than TIEGCM(Weimer). The NH neutral density gap between 2 models decreases beyond 300 km due to temperature and compositional changes.

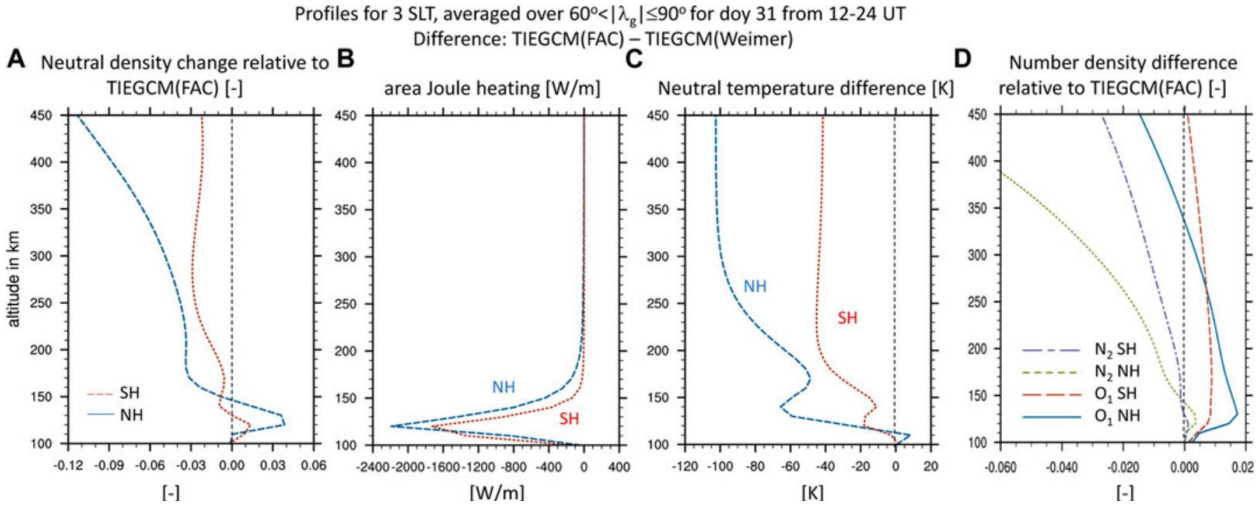

Figure 8: At 3 hours SLT, the profiles of the discrepancies between TIEGCM(FAC) and TIEGCM(Weimer) for the northern hemisphere (dark blue dashed lines) and the southern hemisphere (dark orange dotted lines) averaged between 600 < |λg| ≤ 900 and doy 31.5 to 32.

The southern hemisphere TIEGCM(FAC) so TIEGCM(Weimer) simulations show a smaller negative bias for N2 and a positive bias for O1, and they change less with altitude than the northern hemisphere At practically all altitudes, the TIEGCM(FAC) and TIEGCM(Weimer) simulations show a lower SH than NH neutral density difference. This may be due to the increase in O1 number density, the lesser fall in N2 number density, or the smaller temperature change in SH than NH below 450 km Between 250 and 450 km, the southern neutral density difference is steady, but it should drop beyond 450 km.

Complex dynamical and compositional changes may occur during simple geomagnetically interrupted periods. TIEGCM(Weimer) predicts greater equatorward thermospheric winds in the North Atlantic than TIEGCM(FAC) and poleward winds in subauroral areas. Due to neutral wind changes, the zonal mean atomic oxygen peak travels equatorward from 60 N at quiescent time to 35 N in the TIEGCM(Weimer) simulation. TIEGCM(FAC) simulations only show 45 N movement. The Weimer simulation has less polar atomic oxygen below 350 km than the TIEGCM(FAC) simulation. Comparing TIEGCM(Weimer) with TIEGCM(FAC) simulations shows increased and continuous meridional transfer of atomic oxygen away from the polar area.

Numerous studies have extracted neutral density and quiescent temporal fluctuations from geomagnetic activity. We compute the average quiescent time variation and examine whether decreased atmospheric forcing impacts neutral density. We will eliminate "disturbed" neutral density from average quiescent time latitudinal variation using Climate and WacXBP models.

Figure displays Swarm-C "disturbed" neutral density after eliminating average latitudinal quiescent time shifts from doy 30, 0-22 UT. Doy 32 and 34 stand out in mild geomagnetism, as expected. Simulated quiescent time latitudinal variance is removed by the same manner. Swarm-C neutral density without "disturbed" causes simulation error. When utilizing WacXBP at the lower boundary, TIEGCM(WacXBP) is less inaccurate than Climate.

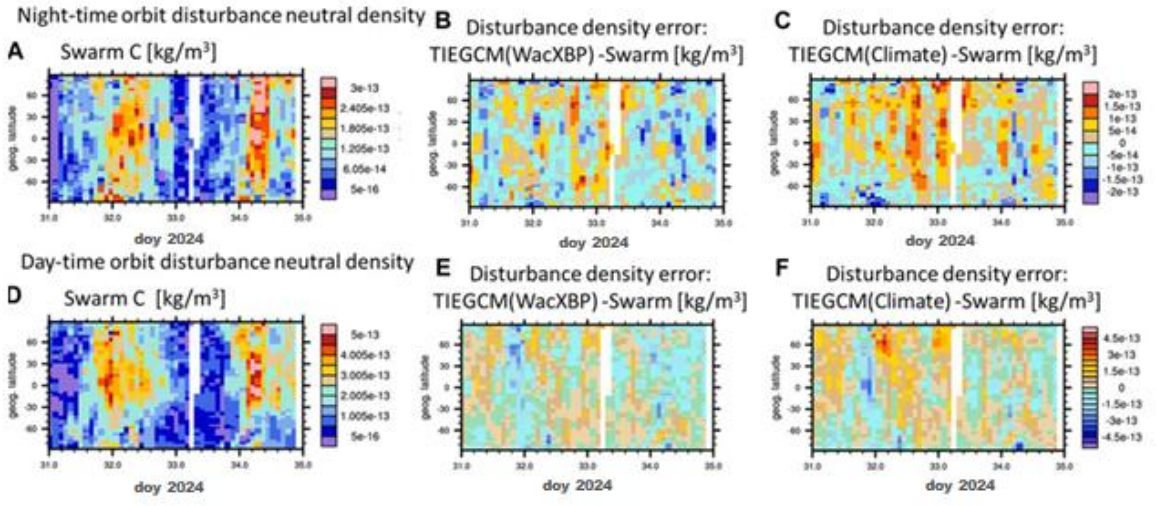

Figure 9: Disturbance neutral density variation for both night-time and day-time orbits of Swarm C, as measured by removing the average of 30 UT 0-21 for both panels (A-C)

and (D) and (F), as well as the difference in disturbance variations between TIEGCM(WacXBP) or Swarm-C (B) & (E), alongside TIEGCM(Climate) & Swarm-C (C) & (F).

CONCLUSION

The study's conclusions show that thermospheric neutral density changes are significantly shaped by both high-latitude magnetospheric inputs and lower atmospheric forcing, which work in concert. In the northern hemisphere, simulations using realistic WACCMX-SD lower boundary conditions reduce density errors by up to 15% and improve agreement with Swarm-C data, particularly at mid- and high latitudes, outperforming those with climatological forcing. It is discovered that the effects of reduced atmospheric variability are highly hemisphere- and altitude-dependent, primarily because of variations in vertical winds, compositional gradients, and tidal influences. Similarly, the use of AMPERE-derived field-aligned currents enhances the depiction of high-latitude energy input, resulting in more accurate density improvements during disturbed times, especially in the dark winter hemisphere when Joule heating effects are more pronounced. The research emphasizes that altitude-dependent compositional behavior, asymmetric heating, and circulation alterations all contribute to interhemispheric asymmetries in density response, which cannot be ascribed to a single cause. Overall, the findings highlight how reliable space weather prediction models and neutral density forecasts—which are essential for satellite operations—can only be achieved by combining realistic high-latitude forcing with correct lower atmospheric dynamics.

References

1. Barth, C. A., Lu, G., & Roble, R. G. (2019). Joule heating and nitric oxide in the thermosphere. *Journal of Geophysical Research: Space Physics*, 114(A5). https://doi.org/10.1029/2008ja013765

2. Billett, D. D., Grocott, A., Wild, J. A., Walach, M. T., & Kosch, M. J. (2018). Diurnal variations in global Joule heating morphology and magnitude due to neutral winds. *Journal of Geophysical Research: Space Physics*. 123(3), 2398–2411. https://doi.org/10.1002/2017ja025141

3. Buonsanto, M. J. (2020). Ionospheric storms—A review. *Space Science Reviews*, 88(3), 563–601. https://doi.org/10.1023/a:1005107532631

4. Cheng, S., Yue, D., Yang, L., & Yue, X. (2017). Dependence of Pedersen conductance in the E and F regions and their ratio on the solar and geomagnetic activities. *Space Weather*, 15(3), 484–494.

5. Crowley, G., Knipp, D. J., Drake, K. A., Lei, J., Sutton, E., & Lühr, H. (2020). Thermospheric density enhancements in the dayside cusp region during strong BY conditions. *Geophysical Research Letters*, 37, L07110. https://doi.org/10.1029/2009GL042143

6. Deng, Y., Fuller-Rowell, T. J., Ridley, A. J., Knipp, D., & Lopez, R. E. (2023). Theoretical study: Influence of different energy sources on the cusp neutral density enhancement. *Journal of Geophysical Research - A: Space Physics*, 118, 2340–2349. https://doi.org/10.1002/jgra.50197

7. Deng, Y., Huang, Y., Lei, J., Ridley, A. J., Lopez, R., & Thayer, J. (2021). Energy input into the upper atmosphere associated with high-speed solar wind streams in 2005. *Journal of Geophysical Research Space Physics*, 116(A5). https://doi.org/10.1029/2010ja016201

8. Doornbos, E., & Klinkrad, H. (2016). Modeling of space weather effects on satellite drag. *Advances in Space Research*, 37(6), 1229–1239. https://doi.org/10.1016/j.asr.2005.04.097

9. Siemes, C., de Teixeira da Encarnação, J., Doornbos, E., van den IJssel, J., Kraus, J., Pereštỳ, R., et al. (2016). Swarm accelerometer data processing from raw accelerations to thermospheric neutral densities. *Earth Planets Space* 68, 92–1186. doi:10.1186/s40623-016-0474-5